Low Energy Electronic Excitations in the Layered Cuprates Studied by Copper L_3 Resonant Inelastic X-Ray Scattering

G. Ghiringhelli,[1] N. B. Brookes,[2] E. Annese,[3] H. Berger,[4] C. Dallera,[1] M. Grioni,[5] L. Perfetti,[5] A. Tagliaferri,[1] and L. Braicovich[1]

[1]*INFM–Dipartimento di Fisica, Politecnico di Milano, Piazza Leonardo da Vinci 32, 20133 Milano, Italy*
[2]*European Synchrotron Radiation Facility, B.P. 220, 38043 Grenoble Cédex, France*
[3]*INFM–Dipartimento di Fisica, Università di Modena e Reggio Emilia, via Campi 213/A, 41100 Modena, Italy*
[4]*IPN, Ecole Polytechnique Fédérale (EPFL), CH-1015 Lausanne, Switzerland*
[5]*Ecole Polytechnique Fédérale (EPFL), CH-1015 Lausanne, Switzerland*

(Received 7 August 2003; published 19 March 2004)

We have measured the resonant inelastic x-ray scattering (RIXS) spectra at the Cu L_3 edge in a variety of cuprates. Exploiting a considerably improved energy resolution (0.8 eV) we recorded significant dependencies on the sample composition and orientation, on the scattering geometry, and on the incident photon polarization. The RIXS final states correspond to two families of electronic excitations, having local (*dd* excitations) and nonlocal (charge-transfer) character. The *dd* energy splitting can be estimated with a simple crystal field model. The RIXS at the L_3 edge demonstrates here a great potential, thanks to the resonance strength and to the large $2p$ spin-orbit splitting.

DOI: 10.1103/PhysRevLett.92.117406 PACS numbers: 78.70.En, 71.70.Ch, 74.72.–h

In recent years considerable effort has been devoted to the study of the very low energy excitations in cuprates superconductors and in other strongly correlated electron systems using high resolution photoemisson. The few meV energy resolution achieved in angle resolved photoemission experiments has allowed accurate *k*-space mapping of the electron-removal excited states, leading to two-dimensional Fermi surfaces in a variety of compounds [1]. On the other hand neutral excitations are harder to access with optical spectroscopies because on-site Cu electronic excitations (the so-called *dd* excitations) are forbidden by electric dipole selection rules. Tanaka and Kotani [2] suggested theoretically that Cu *dd* excitations are potentially accessible with resonant x-ray emission spectroscopy, where the resonant absorption and reemission of an x-ray photon results in the transition of a Cu electron within the $3d$ shell. The process can be seen as a Raman-like scattering of a high energy photon: the energy lost by the photon is transferred to the Cu atom, which is left in an excited state [3,4]. For these reasons the resonant x-ray emission process has been often called resonant Raman x-ray scattering [5,6] or simply resonant inelastic x-ray scattering (RIXS) [7,8]. An accurate mapping of the *dd* excitations and of other few eV neutral excitations (such as those related to the magnetic order) will be of great use for a better understanding of the high T_c superconductors. RIXS spectra and *dd* excitations are an ideal benchmark (different and independent from the photoemission experiments) for calculating the Hamiltonian parameters in the theoretical models dealing with layered cuprates.

The electronic structure of the CuO_2 conduction planes in the cuprates, resulting from the hybridization of the Cu $3d$ atomiclike states with the delocalized O $2p$, can be investigated with resonant x-ray emission in a variety of ways: working at the copper *K* edge [9,10], or at the oxygen *K* edge [11–13], or at the copper $M_{2,3}$ and $L_{2,3}$ edges. The latter cases are potentially very interesting, because the RIXS process involves direct transitions to and from the Cu $3d$ states providing clear information on the charge transfer-, the *dd*-, and the magnetic excitations. Kuiper *et al.* [5] could detect and separate the *dd*- excitations in $Sr_2CuO_2Cl_2$ thanks to the energy resolution of their instrument at the $3p$-$3d$ Cu resonance ($M_{2,3}$ edge). The drawbacks were the insufficient spin-orbit energy separation of the $3p$ states (implying a nonpure intermediate state) and the extreme weakness of the RIXS cross section with respect to the elastic (Rayleigh) scattering, which dominates the experimental spectra. As a consequence the charge-transfer excitations (broader than the *dd*) could not be detected and the lowest energy *dd* excitations got lost in the elastic peak low energy tail. On the other hand a poorer energy resolution at the $L_{2,3}$ edges until now has been an obstacle to the use of RIXS at the $2p$-$3d$ resonance [14–16]. We present RIXS spectra measured in a variety of layered cuprates at the Cu L_3 edge, where the Rayleigh scattering is negligible thanks to the very strong absorption resonance and the 20 eV spin-orbit splitting of the $2p$ ensures a very well defined intermediate state.

The spectra were measured at beam line ID08 of the ESRF (Grenoble, France) using the AXES spectrometer and its dedicated monochromator [17,18]. The incident (emitted) beam energy resolution at 931 eV (Cu^{2+} L_3 peak) was set at 0.7 eV (0.4 eV), resulting in a combined resolution of 0.8 eV FWHM measured on the nonresonant elastic peak. The improvement in the spectrometer performances has been recently obtained by replacing the 2D position sensitive detector [19]. The scattering angle was 70° from the backscattering direction, lying in the

horizontal plane. The linear polarization of the incident beam could be set either perpendicular (vertical polarization, V, hereafter) or parallel (horizontal, H) to the scattering plane. The samples [20,21] were single crystals (except for CuO and La_2CuO_4, which were polycrystalline), cleaved in air in the *ab* plane. The samples could be rotated around a vertical axis in order to have the *c* axis parallel to the incident beam (normal incidence, NI) or at 80° from it (10° grazing incidence, GI). The pressure in the measurement vacuum chamber was better than 5×10^{-8} mbar. All the measurements were made at room temperature. At grazing incidence the surface sensitivity is much smaller in RIXS than in photoemission and we did not notice any evolution of the RIXS spectra during the measurements.

In Fig. 1 we present the Cu L_3 RIXS spectra measured on the insulating compounds CuO, La_2CuO_4, and $Sr_2CuO_2Cl_2$, and on the optimally doped superconductors $La_{1.85}Sr_{0.15}CuO_4$, $Bi_2Sr_2CaCu_2O_{8+\delta}$ (Bi-2212), and $Nd_{1.85}Ce_{0.15}CuO_4$. The experimental setup (grazing incidence and V polarization, [GI,V]) was optimized to minimize the self-absorption, which strongly reduces the elastic peak of the spectra excited at the L_3 peak. As shown in the figure the absorption peak has very little intensity below -1 eV: the RIXS spectra are affected by self-absorption mainly in the first half eV region. The incident photon electric field parallel to the *ab* plane ensures that we fully exploit the absorption resonance [22]. The spectra were aligned with respect to each other within 20 meV by fitting the elastic peak with a Gaussian curve plus a tail from the inelastic peak. The spectra present some common features. The highest energy peak corresponds to elastic or quasielastic scattering (indistinguishable within the experimental energy resolution): its intensity can vary considerably from one sample to another (it is altered by self-absorption, sample orientation, surface roughness, and cleanliness) so we will avoid any discussion on this feature in the following. The main peak around -1.5 to -2 eV, can be assigned to the *dd* excitations [2,14,16]: this peak is clearly different in every sample and is strongly affected by the sample orientation and incident photon polarization, so we will concentrate on it. As a general trend we have observed that the *dd* peak is sharper in the undoped materials, such as La_2CuO_4 and $Sr_2CuO_2Cl_2$, than in the optimally doped $La_{1.85}Sr_{0.15}CuO_4$ and Bi-2212. In particular, La_2CuO_4 and $La_{1.85}Sr_{0.15}CuO_4$ present the *dd* peak at the same energy (around -1.50 eV), but $La_{1.85}Sr_{0.15}CuO_4$ shows a broadening at the base (intensity in a tail around -2.0 to -2.5 eV) which is absent in La_2CuO_4 (see Fig. 2). The low energy tail, extending down to -7 eV and having diverse extension and shape, is given by the charge-transfer excitations.

The basic framework for the interpretation of our RIXS spectra is the following: in undoped materials all the Cu sites are nominally divalent (Cu^{2+}), and copper is

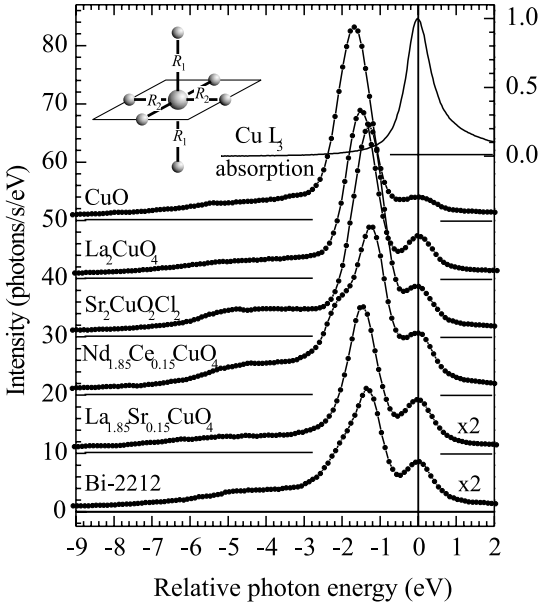

FIG. 1. The RIXS spectra measured at the Cu L_3 peak on three insulating and three superconducting cuprates at grazing incidence and V polarization [GI,V]. The energy scale is given in relative scattered photon energy, having aligned the highest energy peak to zero, by implicitly assigning it to an elastic peak. All the spectra are as measured. The topmost curve shows the Cu L_3 absorption peak of $La_{1.85}Sr_{0.15}CuO_4$. Inset: the local D_{4h} crystal field symmetry used in the calculations.

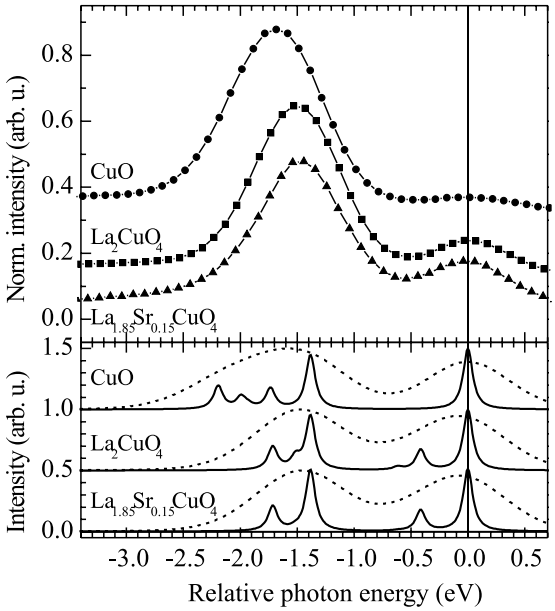

FIG. 2. Upper panel: measured RIXS spectra for CuO, La_2CuO_4, and $La_{1.85}Sr_{0.15}CuO_4$ in [GI,V] geometry. Bottom panel: calculated RIXS spectra in D_{4h} crystal field symmetry. The spectra are given with a 0.05 eV Lorentzian broadening in the final state solid lines) and after a 0.8 eV Gaussian broadening (dashed lines). CuO and La_2CuO_4 are calculated, with the energy parameters of Table I, for a randomly oriented Cu^{2+} ion, $La_{1.85}Sr_{0.15}CuO_4$ in the oriented [GI,V] geometry.

actually in the $\sqrt{x}|3d^9\rangle + \sqrt{1-x}|3d^{10}\underline{L}\rangle$ electronic configuration with $x \simeq 0.6$ [24], where $\underline{L}$ indicates a hole on the neighboring oxygens. There is one hole per Cu, irrespective of the exact value of x that is related to the hybridization of Cu $3d$ and O $2p$ states. In the following we will refer to this hole as a Cu hole, as the excitation energy was chosen to select the $3d^9$ component of the ground state. In all layered cuprates (and practically in CuO as well) every Cu atom is surrounded by four O atoms in a planar 90° coordination (see inset in Fig. 1), whereas the out of plane coordination varies. In all cases the in-plane oxygens are the Cu nearest neighbors, forcing the $3d$ hole to have the x^2-y^2 symmetry proper of the Cu local coordination [22]. The *dd* excitations correspond to the change of the symmetry of the Cu hole from x^2-y^2 to a different one compatible with the local crystalline symmetry, whereas the charge-transfer excitations correspond to the transfer of the Cu $3d$ hole to those states with dominant O $2p$ character. The RIXS process can be summarized as $|3d^9\rangle \rightarrow |2p^3_{3/2}3d^{10}\rangle \rightarrow [|(3d^9)^*\rangle; |3d^{10}\underline{L}\rangle]$: the RIXS spectral distribution gives a direct image of the *dd* excitations, indicated with the $(3d^9)^*$ notation. To make a theoretical prediction of the spectra within a point charge crystal field model we have calculated the energies of the final states (*dd*-excitation energies) and all the transition probabilities in the given experimental conditions (sample orientation, scattering angle, and photon polarization).

We present here calculations for tetragonally distorted octahedral symmetry: CuO (locally), $La_{2-x}Sr_xCuO_4$ and $Sr_2CuO_2Cl_2$. In those materials the in-plane Cu-O distances are very similar (1.92, 1.89, and 1.94 Å for CuO, $La_{2-x}Sr_xCuO_4$, and $Sr_2CuO_2Cl_2$, respectively), whereas there are two apical O at 2.43 Å in $La_{2-x}Sr_xCuO_4$, two apical Cl at 2.86 Å in $Sr_2CuO_2Cl_2$, and no apical atoms in CuO. The local symmetry is thus D_{4h} (tetragonally distorted octahedron) in all cases, and the commonly used set of atomic d states are well suited to represent the *dd* excitations in terms of transfer of the $3d$ hole from the x^2-y^2 orbital (b_{1g}) to the z^2 (a_{1g}), xy (b_{2g}), yz (e_g) or zx (e_g) orbitals. We notice that there is only one intermediate state ($|2p^3_{3/2}3d^{10}\rangle$) in the RIXS process, and only $5 + 5$ final states (the five orbitals split by the superexchange interaction). The energy sequence is not unique, and depends on the tetragonal distortion; in the absence of any distortion one finds the O_h symmetry, characterized by the $10Dq$ parameter [23]. Three quantities are used to describe the single particle energy levels in D_{4h} symmetry: $10Dq_{R2}$, D_s, and D_t. We have used the method presented in Ref. [23] to calculate the parameters of CuO, $La_{2-x}Sr_xCuO_4$, and $Sr_2CuO_2Cl_2$, using the R_1 and R_2 distances shown in the inset of Fig. 1, a $-2e$ point charge for oxygen and a $-e$ point charge for chlorine. The energies given by the algorithm required a slight optimization only in the case of $Sr_2CuO_2Cl_2$. The results are summarized in Table I, where the energies of the different orbitals are referred to the b_{1g} state, the highest in energy and thus the one occupied by the hole in the ground state. We notice here that $10Dq_{R2} = 1.29$ eV for $Sr_2CuO_2Cl_2$ is slightly different from the 1.35 eV of Ref. [5]. Finally each final state is further split by the superexchange interaction (the spin flip energy is set to $\Delta_{SF} = 0.20$ eV in our simulations as in Ref. [5]).

TABLE I. Parameters calculated with the crystal field model of Ref. [23]. The relations between the crystal field parameters and the state energies are $E(b_{1g}) = \frac{3}{5}(10Dq_{R2}) + 2D_s - D_t$, $E(a_{1g}) = \frac{3}{5}(10Dq_{R2}) - 2D_s - 6D_t$, $E(b_{2g}) = -\frac{2}{5}(10Dq_{R2}) + 2D_s - D_t$, and $E(e_g) = -\frac{2}{5}(10Dq_{R2}) - D_s + 4D_t$. In this table the energy positions of a_{1g}, b_{2g}, and e_g are referred to the energy of b_{1g}.

	CuO	$La_{2-x}Sr_xCuO_4$	$Sr_2CuO_2Cl_2$
$10Dq_{R2}$	1.38 eV	1.38 eV	1.29 eV
D_s	0.33 eV	0.08 eV	0.22 eV
D_t	0.08 eV	0.02 eV	0.05 eV
a_{1g} $[z^2]$	−1.73 eV	−0.41 eV	−1.17 eV
b_{2g} $[xy]$	−1.38 eV	−1.38 eV	−1.29 eV
e_g $[yz; zx]$	−1.99 eV	−1.51 eV	−1.69 eV

Once the final state energies are known the scattering probabilities are obtained with the Kramers-Heisenberg (KH) formula [25], computed using the single particle matrix elements by taking into account the scattering conditions. We have to consider four combinations of incident/emitted photon polarizations. In the experiment the scattered photons polarization was not detected, so also in the calculations the final spectral intensities are given by the sums over the emitted photon polarizations. The considered geometrical setup is reported in the inset of Fig. 3. The single crystalline sample has the a, b, and c axes oriented as x, y, and z, respectively. We recall here that the charge-transfer excitations are not included in our calculations.

Tanaka and Kotani [2] first suggested measuring Cu L_3 RIXS spectra of CuO and La_2CuO_4 , to test the capability of this technique to probe the energy distribution of *dd* excitations. By applying the Anderson impurity model they predicted that the average energy of the *dd* excitation should be higher (meaning a bigger separation of the main peak from the elastic peak) in La_2CuO_4 than in CuO. However, our experimental results, reported in the upper panel of Fig. 2, clearly show the opposite: the main peak is at −1.50 eV for $La_{2-x}Sr_xCuO_4$ and −1.70 eV for CuO. Moreover, our crystal field model calculations are in good agreement with the measured spectra as shown in the bottom panel of Fig. 2 (the elastic peak intensities cannot compare due to the self-absorption in the experimental data).

In Fig. 3 we show the effect of the incident photon polarization on the $Sr_2CuO_2Cl_2$ spectra. The three spectra are obtained with the electric field of the incident photons lying in the ab plane, and the difference comes from the orientation of the emitted photons with respect to the c axis (if we compare the [GI,V] and [NI,V] cases) or with

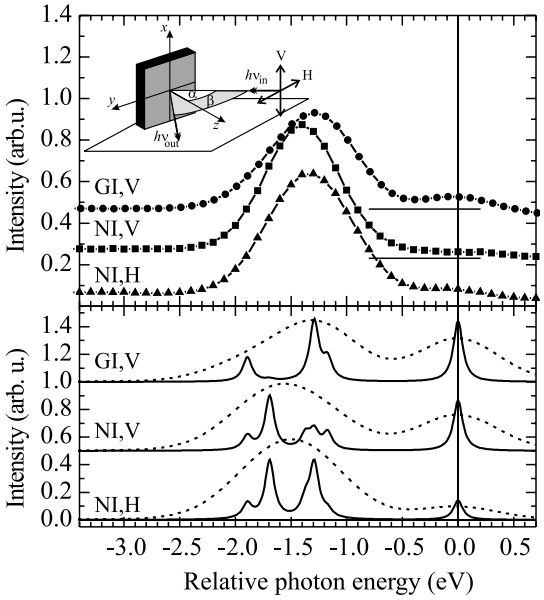

FIG. 3. Upper panel: RIXS spectra of $Sr_2CuO_2Cl_2$ measured at grazing and normal incidence with V and H polarizations ([GI,V], [NI,V], [NI,H]). Bottom panel: calculated spectra for the same scattering geometries. Inset: experimental geometry, where $\beta = 70°$ is the scattering angle and $\alpha = 0°$ (80°) is the incidence angle in the NI (GI) configuration.

respect to the incident polarization ([NI,V] and [NI,H] cases). It must be considered that at normal incidence the self-absorption of the elastic peak is much stronger that at grazing incidence. The calculations (lower panel), made for the very same geometry of the experiment, can account for those polarization effects. In reference [5] the [GI,V] and [NI,V] comparison was already made, whereas the differences between [NI,V] and [NI,H] are shown here for the first time. This effect has to be ascribed to the polarization of the intermediate state detected through the second order process described by the KH formula. On the contrary in a two step model the difference vanishes. When comparing [NI,V] and [NI,H] the experimental geometry is the same and the spectral differences cannot be attributed to self-absorption.

In conclusion, we have measured Cu L_3 RIXS spectra of cuprates that allow a systematic comparison of different samples. Both the *dd* and charge-transfer excitations are present in all the spectra. Although we could reproduce the *dd*-excitation peak using a simple crystal field model, also more sophisticated calculations can greatly benefit from comparison with the experimental results presented here. For example, the predictions of Ref. [2], made with the Anderson impurity model, do not agree with the experimental findings, whereas our calculations show a better agreement. We found also that in $La_{1.85}Sr_{0.15}CuO_4$ the RIXS spectra are relatively insensitive to the doping level, probably because the excitation energy acts as a selector of the $3d^9$ part of the ground state. The polarization dependence of the spectra, useful to assigning the symmetry of the final states, in some cases is a signature of the second order nature of the scattering process. The potential of Cu RIXS had been previously demonstrated by Kuiper *et al.* [5] at the $M_{2,3}$ edges of Cu. Our data show that, thanks to the recent progress in the instrumentation, L_3 RIXS has become a very precious spectroscopic tool as well. Ultimately, the unambiguous separation of the different components in the neutral excitation spectrum will be probably obtained only by combining the data at the *K*, *L*, and *M* edges, giving access to the charge transfer, the *dd*-, and the very low energy excitations, respectively.

We gratefully acknowledge L. H. Tjeng, A. A. Menowsky, and O. Tjernberg for making their samples available.

[1] A. Damascelli *et al.*, Rev. Mod. Phys. **75**, 473 (2003).
[2] S. Tanaka and A. Kotani, J. Phys. Soc. Jpn. **62**, 464 (1993).
[3] S. M. Butorin *et al.*, Phys. Rev. B **54**, 4405 (1996).
[4] F. Gel'mukhanov and A. Agren, Phys. Rev. A **54**, 3960 (1996).
[5] P. Kuiper *et al.*, Phys. Rev. Lett. **80**, 5204 (1998).
[6] P. Carra *et al.*, Phys. Rev. Lett. **74**, 3700 (1995).
[7] M. H. Krisch *et al.*, Phys. Rev. Lett. **74**, 4931 (1995).
[8] G. P. Zhang *et al.*, Phys. Rev. Lett. **88**, 077401 (2002).
[9] J. P. Hill *et al.*, Phys. Rev. Lett. **80**, 4967 (1998).
[10] K. Tsutsui *et al.*, Phys. Rev. Lett. **83**, 3705 (1999).
[11] L. C. Duda *et al.*, Phys. Rev. B **61**, 4186 (2000).
[12] J.-H- Guo *et al.*, Phys. Rev. B **61**, 9140 (2000).
[13] Y. Harada *et al.* Phys. Rev. B **66**, 165104 (2002).
[14] K. Ichikawa *et al.*, J. Electron Spectrosc. Relat. Phenom. **78**, 183 (1996).
[15] L. C. Duda *et al.*, J. Phys. Soc. Jpn. **67**, 416 (1998).
[16] L. C. Duda *et al.*, J. Electron Spectrosc. Relat. Phenom. **110–111**, 275 (2000).
[17] C. Dallera *et al.*, J. Synchrotron Radiat. **3**, 231 (1996).
[18] G. Ghiringhelli *et al.*, Rev. Sci. Instrum. **69**, 1610 (1998).
[19] An in vacuum CCD for soft x rays has replaced the previous microchannel plate based detector: M. Di Nardo *et al.* (unpublished).
[20] T.W. Li *et al.*, J. Cryst. Growth **135**, 481 (1994).
[21] The $Sr_2CuO_2Cl_2$ samples were prepared at the EPFL: A. B. Bykov *et al.*, J. Cryst. Growth **139**, 81 (1994).
[22] C. T. Chen *et al.*, Phys. Rev. Lett. **68**, 2543 (1992).
[23] I. B. Bersuker, *Electronic Structure and Properties of Transition Metal Compounds* (John Wiley, New York, 1996).
[24] H. J. Eskes *et al.*, Phys. Rev. B **41**, 288 (1990).
[25] F. M. F. de Groot *et al.*, Phys. Rev. B **57**, 14 584 (1998).